

Subthreshold \bar{p} production in pC , dC and αC reactions

H. Müller

Institut für Kern- und Hadronenphysik, Forschungszentrum Rossendorf, Postfach 510119, D-01314 Dresden, Germany^{*}

V. I. Komarov

Joint Institute for Nuclear Research, LNP, 141980 Dubna, Russia[†]

(Dated: December 2, 2024)

Data from KEK on subthreshold \bar{p} as well as on π^\pm and K^\pm production in pC , dC and αC reactions at energies between 3.5 and 12.0 AGeV are described for the first time within a unified approach. We use a model which considers a nuclear reaction as an incoherent sum over collisions of varying numbers of projectile and target nucleons. It samples complete events and allows thus for the simultaneous consideration of all final particles including the decay products of the nuclear residues. The enormous enhancement of the \bar{p} cross section as well as the moderate increase of meson production in dC and αC compared to pC reactions is well reproduced. In our approach the observed enhancement near the production threshold is mainly due to the contributions from the interactions of few-nucleon groups.

PACS numbers: 24.10.-i; 24.10.Lx; 25.40.-h; 25.45.-z; 25.55.-e

I. INTRODUCTION

Subthreshold particle production in a nuclear reaction is understood as production below the energy threshold of the considered process in a free nucleon-nucleon (NN) collision. It is thus a nuclear phenomenon which may be explained by rather different assumptions on the properties of nuclear matter and on the interaction dynamics. The energy available for particle production can be increased using high-momentum components in the nuclear wave function caused by short-range correlations. Also the assumption of a collective behaviour of several target nucleons, either mediated by various kinds of intermediate particles or caused by local density fluctuations, increases the available energy. On the other hand, the properties of hadrons may become modified in the nuclear medium leading to an efficient decrease of the particle production threshold if the mass of the considered hadron decreases accordingly. It is an open question to what extent subthreshold particle production is governed by properties of the nuclear ground state wave function and to what extent by the dynamical properties of nuclear matter, not reflected in the ground state description. The problem is far from a final solution at present and evidently requires a systematic study of high-momentum transfer processes, among them subthreshold particle production.

First measurements of subthreshold \bar{p} production in proton-nucleus collisions had been carried out [1, 2, 3, 4] a few decades ago. Then investigations in nucleus-nucleus collisions [5, 6, 7, 8, 9] and more recent studies of proton-nucleus reactions [10] followed. In [11] for the first time light-ion induced \bar{p} production has been investigated and

an enormous enhancement of subthreshold \bar{p} production in deuteron-nucleus reactions compared to proton-nucleus interactions has been found. This fact has been confirmed by the final results of the KEK group [12]. They measured d - and α -induced reactions in the energy region between 2.5 and 5.0 GeV/nucleon and observed at 3.5 GeV/nucleon an \bar{p} cross sections nearly two and three orders of magnitude larger than measured in proton-nucleus reactions.

Most of the descriptions proposed so far are based on transport calculations [13, 14, 15, 16, 17, 18, 19, 20, 21, 22], thermodynamical considerations [23, 24, 25, 26] or multi-particle interactions [27] and are devoted to proton and/or heavy-ion induced reactions. By measuring light-ion induced subthreshold \bar{p} production the KEK group [12] intended to provide an experimental test for models in this transition region between proton and heavy-ion induced reactions. To the best of our knowledge only one paper [19] has been published so far, which compares proton- and deuteron-induced \bar{p} production at subthreshold energies.

It should be stressed that all mentioned papers on subthreshold \bar{p} production consider the \bar{p} spectra without any relation to results concerning other reaction channels. At KEK [12], however, the spectra of π^\pm and K^\pm mesons were measured together with those of the antiprotons. In a recent paper [28] we considered in the framework of the Rossendorf collision (ROC) model simultaneously all these reaction channels for pC reactions and achieved a good reproduction of the data. In the present paper we extend these considerations to dC and αC reactions using the same parameter set.

In the ROC-model it is assumed that the nuclear residue becomes excited during the reaction due to the distortion of the nuclear structure by the separation of the participants from the spectators and due to the passage of the reaction products through the spectator system. In this way final-state interactions are taken into

^{*}Electronic address: H.Mueller@fz-rossendorf.de

[†]Electronic address: komarov@nusun.jinr.ru

account without making for each particle type special assumptions concerning re-absorption, re-scattering, self-energies, potentials etc. (see also [28]). The fragmentation of the residual nuclei and the interaction of the nucleons participating in the scattering process are treated on the basis of analogous assumptions. Even more important, the phase-space of the complete final state consisting of the reaction products of the interaction of the participants as well as the fragments of the decay of the spectator systems is exactly calculated. This feature seems to be unique to the ROC-model.

The plan of the paper is as follows. In sect. II the main ingredients of the ROC-model are explained, which is used for the calculations to be presented. Section III contains a comparison of theoretical and experimental results for particle production with special emphasis put on subthreshold \bar{p} production. A summary is given in sect. IV.

II. THE MODEL

The ROC-model is implemented as a Monte-Carlo generator which samples complete events for hadronic as well as nuclear reactions. It makes no detailed assumptions on the intra-nuclear development of the interaction process, but calculates instead the statistical weights of the possible final states. The dynamics of the reaction is taken into account in form of empirical functions which modify the population of the final states. This is in contrary to transport models, where the interaction of the projectile with target nucleons and the subsequent interactions of particles originating from primary collisions with further target nucleons are modelled. The ROC-approach does not need any parameterisations of elementary cross sections. Its applicability is not restricted at higher energies by the growing number of unknown elementary cross sections. All dynamic information is gathered in a few parameters which are either constant or change smoothly with energy and/or target mass. The energy necessary for subthreshold production stems from interactions of few-nucleon groups, also called clusters in the following, and from the Fermi motion of these clusters.

The model was successfully tested for pp interactions up to ISR energies in [29, 30], while nuclear reactions were considered in the papers [28, 31, 32, 33, 34]. In the following the basic ideas of the ROC-model are summarised. Although we consider in the present paper only light-ion induced reactions the given presentation is applicable to any nucleus-nucleus reaction.

The cross section of the interaction of two nuclei $(\mathcal{A}, \mathcal{Z}_A)$ and $(\mathcal{B}, \mathcal{Z}_B)$ characterised by their mass and charge numbers is considered as an incoherent sum over contributions from varying numbers a and b of nucleons (thereof z_a and z_b protons) participating in the interac-

tion

$$d\sigma(s) = \sum_{a=1}^{\mathcal{A}} \sum_{z_a=\max(0, a-\mathcal{Z}_A)}^{\min(a, \mathcal{Z}_A)} \sum_{b=1}^{\mathcal{B}} \sum_{z_b=\max(0, b-\mathcal{Z}_B)}^{\min(b, \mathcal{Z}_B)} \sigma_{az_abz_b} \frac{dW(s; \boldsymbol{\alpha}_{az_abz_b})}{\sum_{\boldsymbol{\alpha}_{az_abz_b}} dW(s; \boldsymbol{\alpha}_{az_abz_b})}. \quad (1)$$

Here, $s = P^2$ denotes the square of the centre-of-mass energy of the projectile-target system and $P = (E, \vec{P})$ the total four-momentum. The partial cross sections $\sigma_{az_abz_b}$ are calculated using a modified version of a Monte-Carlo code [35] which is based on a probabilistic interpretation of the Glauber theory [36] in close analogy to [37, 38]. We use the profile function

$$\Gamma_{\mathcal{A}\mathcal{B}}(d) = \int \left[1 - \prod_{i=1}^{\mathcal{A}} \prod_{j=1}^{\mathcal{B}} (1 - p_{ij}) \right] \prod_{i=1}^{\mathcal{A}} \rho_{\mathcal{A}}(\vec{r}_i) d^3 r_i \prod_{j=1}^{\mathcal{B}} \rho_{\mathcal{B}}(\vec{r}_j) d^3 r_j$$

of the considered nuclei, which depends on the nucleon densities $\rho_{\mathcal{A}}(\vec{r}_i)$, $\rho_{\mathcal{B}}(\vec{r}_j)$ and the probability

$$p_{ij} = \exp(-d_{ij}^2 \pi / \sigma_{NN})$$

for an interaction of the i -th projectile and the j -th target nucleon with d_{ij} being the distance between the interacting particles. The nucleon density [39]

$$\rho_{\mathcal{A}}(\vec{r}) \propto (1 + \eta [1.5(f^2 - e^2)/f^2 + e^2 r^2/f^4]) \exp(-r^2/f^2) \quad (2)$$

of light nuclei $2 < \mathcal{A} < 20$ can be derived from a standard shell model wave function with $\eta = (\mathcal{A} - 4)/6$, $f^2 = e^2(1 - 1/\mathcal{A})$ and $f = 1.55$ fm. For the deuteron the Paris deuteron wave function [40] is used. Then the NN cross section σ_{NN} is adapted such that the integral of the profile function over the impact parameter d reproduces the total inelastic $\mathcal{A}\mathcal{B}$ cross section

$$\sigma_{\mathcal{A}\mathcal{B}}^{in} = \int d^2 d \Gamma_{\mathcal{A}\mathcal{B}}(d).$$

The same calculation yields also the partial cross sections $\sigma_{az_abz_b}$ we are interested in (for further details see [35]).

In (1), the quantities

$$dW(s; \boldsymbol{\alpha}_{az_abz_b}) \propto dL_n(s; \boldsymbol{\alpha}_{az_abz_b}) \rho_{\mathcal{A}}(\vec{P}_A) \rho_{\mathcal{B}}(\vec{P}_B) T^2 \quad (3)$$

describe the relative probabilities of the various final channels $\boldsymbol{\alpha}_{az_abz_b}$. They are given by the Lorentz-invariant phase-space factor $dL_n(s; \boldsymbol{\alpha}_{az_abz_b})$ multiplied by the square of the empirical reaction matrix element T^2 describing the collision dynamics. The Fermi motion is implemented via the momentum distributions of the residual nuclei $\rho_{\mathcal{A}}(\vec{P}_A)$ and $\rho_{\mathcal{B}}(\vec{P}_B)$, which are made functions of the numbers a and b of participants. They

are taken as Gaussians having in case of nucleus \mathcal{A} a width of

$$\sigma_a = \sqrt{aA/5/(\mathcal{A}-1)} p_F \quad (4)$$

in accordance with the independent particle model [41] with $A = \mathcal{A} - a$ being the number of nucleons in the residue and p_F is the Fermi-limit of the nucleus considered. For nucleus \mathcal{B} an analogous formula holds, and for the deuteron again the Paris deuteron wave function [40] is employed, now in momentum space. No special high-momentum component [42, 43, 44, 45, 46, 47] is used in the present paper in order to avoid additional uncertainties.

The Lorentz-invariant phase-space is defined as the integral over the three-momenta of the n primarily produced final particles with energy-momentum conservation taken into account

$$dL_n(s; \alpha_{az_a b z_b}) = \prod_{i=1}^n \frac{d^3 p_i}{2e_i} \delta^4(P - \sum_{i=1}^n p_i), \quad (5)$$

Here, the four-momentum of the i -th particle is denoted by $p_i = (e_i, \vec{p}_i)$ with $p_i^2 = m_i^2$.

For numerical calculations the δ -function in eq. (5) has to be removed by introducing a new set of $3n - 4$ variables to replace the $3n$ three-momentum components. It is reasonable to choose a set of variables, which reflects the underlying physical picture of the interaction process. Using recursion [48] eq. (3) can be rewritten in the form

$$dW(s; \alpha_{az_a b z_b}) \propto \frac{d^3 P_A}{2E_A} \rho_{\mathcal{A}}(\vec{P}_A) \frac{d^3 P_B}{2E_B} \rho_{\mathcal{B}}(\vec{P}_B) dW_A(M_A^2) dW_B(M_B^2) dW_C(M_C^2) \quad (6)$$

with the four-momenta of the nuclear residues $P_A = (E_A, \vec{P}_A)$, $P_B = (E_B, \vec{P}_B)$ and of the participants

$$P_C = P - P_A - P_B = (E_C, \vec{P}_C), \quad (7)$$

the corresponding invariant masses are given by $M_A^2 = P_A^2$, $M_B^2 = P_B^2$ and $M_C^2 = P_C^2$. The integrals over the Fermi motion $d^3 P_A \rho_{\mathcal{A}}(\vec{P}_A)/2E_A$ and $d^3 P_B \rho_{\mathcal{B}}(\vec{P}_B)/2E_B$ separate in accordance with the participant-spectator picture the phase-spaces of the n_A and n_B nuclear fragments

$$\begin{aligned} dW_A(M_A^2) &= dM_A^2 dL_{n_A}(M_A^2) T_A^2 \\ dW_B(M_B^2) &= dM_B^2 dL_{n_B}(M_B^2) T_B^2 \end{aligned} \quad (8)$$

from the phase-space

$$dW_C(M_C^2) = dL_{n_C}(M_C^2) T_C^2 \quad (9)$$

of the $n_C = n - n_A - n_B$ final particles arising from the participant system. In (8) and (9) the matrix element $T^2 = T_A^2 T_B^2 T_C^2$ is split into factors describing residue fragmentation (T_A^2 and T_B^2) and participant interaction (T_C^2). There is, however, a strong kinematic

link between participants and spectators, since invariant mass M_C of the participant system, invariant masses M_A and M_B of the residues and the relative kinetic energy $\sqrt{s} - M_A - M_B - M_C$ of these three particle groups are connected by energy-momentum conservation. For particle production to proceed the invariant mass of the participants must exceed the corresponding threshold value M_C^{th} which in turn depends on the number of participants. The heavier the effective target is the more energy is available for particle production. Another way to reach the threshold value goes via the Fermi motion, since the participant mass is a function of the momentum vector of the nuclear residue. The excitation energy of the target residue comes usually into play via the spectral function (see *e.g.* [44]) derived from electron scattering data. Unique to the ROC-model, however, is the treatment of the spectator system in close analogy to the participant subsystem. The ROC-model calculates the complete final state of both the participants and the spectators. Thus, the huge amount of final channels of the spectator fragmentation influences directly the final state of the participant system and vice versa.

The term $dW_C(M_C^2)$ in (6), (9) describes the interaction of the groups of participating nucleons. Such a cluster-cluster reaction is treated in complete analogy to a hadronic reaction. In a first step intermediate particle groups called fireballs (FBs) are produced, which decay into so-called primary particles. The primary particles define the channels for which the weights (9) are calculated. Among them are resonances, which decay subsequently into stable hadrons. The dynamical input of the cluster-cluster reaction is implemented by the empirical transition matrix element

$$T_C^2 = T_i^2 T_{qs}^2 T_{ex}^2 T_t^2 T_l^2 T_{st}^2, \quad (10)$$

which describes the interaction process T_i^2 resulting in the production of $N \geq 2$ FBs, the production of hadrons T_{qs}^2 via the creation of quark-anti-quark ($q\bar{q}$) pairs, the invariant-mass distribution of the FBs T_{ex}^2 , the transverse T_t^2 and longitudinal T_l^2 momentum distribution of the FBs, and, finally, some factors T_{st}^2 necessary for the calculation of the statistical weights. The interaction is assumed to proceed via colour exchange leading to the removal of valence quarks or of gluons from the interacting hadrons. Additional up, down and strange quark pairs are created in the ratio

$$u : d : s = 1 : 1 : \lambda_s \quad (11)$$

with $\lambda_s = 0.15$. They form the varying number of FBs, which subsequently decay into the final hadrons. The transverse momenta P_t of the FBs are restricted by an exponential damping (longitudinal phase-space) according to

$$T_t^2 = \prod_{I=1}^N \exp(-\gamma P_{t,I}) \quad (12)$$

with the mean $\bar{P}_t = 2/\gamma$. Two leading FBs, the remnants of the incoming clusters, get in the mean larger longitudinal momenta than the central FBs by weighting the events with

$$T_1^2 = (X_1 X_2)^\beta. \quad (13)$$

Here, the light-cone variables $X_1 = (E_1 + P_{z,1})/(e_a + p_{z,a})$ and $X_2 = (E_2 - P_{z,2})/(e_b + p_{z,b})$ are used with the four-momenta of the participants given by $p_a = (e_a, \vec{p}_a)$ and $p_b = (e_b, \vec{p}_b)$. Each FB is characterised by two parameters, a temperature Θ_{FB} and a volume V_{FB} . The temperature determines the relative kinetic energy of the particles the FB decays into via

$$T_{ex}^2(\Theta_{FB}) = \prod_{I=1}^N (M_I / \Theta_{FB}) K_1(M_I / \Theta_{FB}), \quad (14)$$

while the volume defines the interaction region and influences mainly the particle multiplicity via the statistical factor $T_{st}^2 \propto V_{FB}^{n_C - 1}$. In (14) K_1 stands for the modified Bessel function. Final hadrons are built-up by random recombination of the available quarks during the decay of the FBs. This procedure ensures automatically the conservation of all internal quantum numbers. Subsequently resonances decay until the final state consisting of stable particles is reached. For a more detailed discussion of the hadronic matrix element the reader is referred to [30]. In the present paper we use the same set of parameters as in [30] for the description of the interaction of a single projectile nucleon with a single target nucleon. Most of the other terms in (1), however, contain clusters consisting of several nucleons. The basic parameters of the FBs emerging from such an interaction are fixed by scaling the volume and the temperature parameter according to

$$V_{FB} = V_{FB}^0 (a+b-1) \quad \text{and} \quad \Theta_{FB} = \Theta_{FB}^{max} (a+b-1)^{-1/3}. \quad (15)$$

It remains to consider the target residues, the structure of which is strongly disturbed by the interaction of the participants and subsequent final-state interactions. This leads to the excitation and decay of the spectator systems, which are characterised by the two parameters temperature Θ_R and volume V_R ($R = A$ or B in dependence on the residue under consideration) in the same way as the FBs emerging from the participant interaction. The part of the matrix element responsible for the residue fragmentation

$$T_R^2(\alpha_{az_a bz_b}^R) = T_{ex}^2(\Theta_R) T_{st}^2(\alpha_{az_a bz_b}^R) \quad R = A, B$$

is identical with the corresponding factors (10) applied to the hadronic FBs. In order to restrict the excitation energy transferred to the residue we use the asymptotic approximation of (14) for large mass and small temperature

$$T_{ex}^2(\Theta_R) = \sqrt{M_R / \Theta_R} \exp(-M_R / \Theta_R) \quad R = A, B. \quad (16)$$

An impact parameter dependence is assumed for the temperature parameter. This seems to be reasonable, because a peripheral collision with only few participating nucleons should excite the nuclear residue much less than a central collision with many participants. As a first guess we use

$$\begin{aligned} \Theta_A &= \Theta_A^{max} [1 - \exp(-a/\bar{a}A^{1/3})] \\ \Theta_B &= \Theta_B^{max} [1 - \exp(-b/\bar{a}B^{1/3})] \end{aligned} \quad (17)$$

with \bar{a} as parameter, here fixed to $\bar{a} = 0.5$, which determines how fast the maximal temperatures Θ_A^{max} and Θ_B^{max} are reached with increasing number of participants. The value $\Theta_A^{max} = \Theta_B^{max} = 12$ MeV has been fixed in [28] from a comparison of the energy spectra of fragments from the reaction of 2.1 GeV protons with carbon measured at 90° [49] with ROC-model calculations.

All factors still necessary for a correct calculation of the relative weights of the various channels are collected in complete analogy to the corresponding factors for the FBs in the product of two terms with $R = A$ and $R = B$ according to

$$T_{st}^2(\alpha_{az_a bz_b}^R) = g(\alpha_{az_a bz_b}^R) \left(\frac{V_R}{(2\pi)^3} \right)^{n_R - 1} \prod_{i=1}^{n_R} (2\sigma_i + 1) 2m_i. \quad (18)$$

It contains the spin degeneracy factors $(2\sigma_i + 1)$ and the volume V_R in which the particles are produced. The quantity $g(\alpha_{az_a bz_b}^R)$ is the degeneracy factor for groups of identical particles in the final state of the residue decay and prevents multiple counting of identical states.

As in the case of hadronic reactions, temperature and volume determine the number of final particles and their relative energy. The main difference consists in the value of the temperature parameter, $\Theta_{FB}^{max} \approx 300$ MeV for hadronic and $\Theta_R^{max} \approx 10$ MeV for nuclear systems. New particles can be produced in hadronic reactions, while for nuclear systems, due to the much lower temperature, the nucleons of the initial state are recombined into various fragments without producing new hadrons. The volume parameter defines the distance between the fragments where the strong interaction ceases to work. This volume is introduced into the calculation of the weight of the final state. Due to the long range of the Coulomb repulsion Coulomb energy is still stored in the system at those distances. This energy is calculated in the Wigner-Seitz-approximation (see [50]). The random distribution of the Coulomb energy among the charged fragments yields the final momenta of the fragments at large distances.

In the calculation we assume that the fragments emerging from the residues are stable against particle decay. The possibility of hot fragments cooling down by subsequent particle emission is also implemented in the model (see [31]), but it turned out that a readjustment of the volume and/or the temperature parameter yields quite similar results in both cases. So we decided in favour of the easier approach.

III. COMPARISON WITH EXPERIMENTAL DATA

In fig. 1 the momentum spectra of π^\pm , K^\pm and \bar{p} from pC , dC and αC reactions measured at KEK [12] are displayed. The experimental efforts of the KEK group were motivated by measurements of large cross sections of sub-threshold \bar{p} production in nucleus-nucleus reactions at LBL-BEVALAC [6, 7] and at GSI [8]. The authors [12] claimed that the use of light-ion beams for investigating subthreshold \bar{p} production should be useful to verify theoretical models. Secondary effects like re-scattering, re-absorption, self-energies, potentials etc., which hide and influence features of the primary production process, should be smaller than in heavy-ion reactions. Indeed, it is the outstanding feature of the data that in d - and α -induced reactions an enormous enhancement of \bar{p} production by nearly two and three orders of magnitude compared to p -induced interactions could be observed. The very fact of finding this enhancement in light-ion induced reactions makes this interaction type a candidate for the key to a deeper understanding of subthreshold \bar{p} production in nucleus-nucleus reactions.

The KEK group [12] interprets their \bar{p} data by using the “first-chance NN collision model” from [42] where the internal nucleon momenta were extracted from backward proton production [43] as a superposition of two Gaussian distributions. In this way the momentum spectra and the incidence-energy dependence of p -induced reactions could be successfully reproduced by adapting one normalisation parameter. However, the application of this model to d -induced reactions using different deuteron wave-functions and the normalisation from p -induced interactions severely underestimates the \bar{p} cross sections at subthreshold energies. Thus, according to [12], the effect cannot be explained by the internal motion of the nucleons in the deuteron, even if a deuteron wave-function with a high-momentum component is used.

In [19] \bar{p} production in $p + A$ and $d + A$ reactions is analysed within a phase-space model incorporating the self-energies of the baryons. Here, it is claimed that the internal momentum distribution of the deuteron provides a natural explanation of the large enhancement under discussion.

To the best of our knowledge there is no paper which describes the further increase of subthreshold \bar{p} production in α -induced reactions. Thus, the approach presented here seems to be the first attempt to consider the whole set of projectiles in a unified picture. Beyond it, we also regard the whole set of ejectiles measured. This is of special importance since there is not only the enhancement of \bar{p} production, but also the increase of the K^- cross sections with increasing energy and mass number of the projectile around the elementary production threshold at 2.6 GeV. And also the completely different energy and projectile-mass dependence of the pion production cross sections far above the threshold should be explained by a realistic approach.

In fig. 1 the results of the ROC-model calculated with one fixed parameter set are compared to the data [12]. The overall agreement is quite satisfactory in view of the different projectile types, the large region of incidence energies, the variety of ejectile species and the huge differences of many orders of magnitude in the considered cross section values. Particle yields are influenced by the suppression factor $\lambda_s = 0.15$, eq. (11), of strange quarks and by the algorithm for creating the final hadrons from the quarks produced in the first stage of the interaction process. Hadrons are built up in each FB independently according to the rules of quark statistics [51] by randomly selecting sequences of q ’s and \bar{q} ’s. A $q\bar{q}$ gives a meson, while baryons or antibaryons are formed from qqq or $\bar{q}\bar{q}\bar{q}$. From a given sequence of quarks the different hadrons are formed according to the tables of the particle data group [52]. There is no parameter which directly determines the ratio between meson and baryon production as *e.g.* in the PYTHIA-LUND model [53, 54, 55, 56]. Only an indirect influence via the temperature and the volume parameter is possible, which change the relative weights of the FBs in dependence on their invariant mass and final particle multiplicity, respectively.

It is, therefore, remarkable that the general trend of the energy dependence of the data for all projectile types, moderate increase with energy of the cross sections for the light mesons and steep increase of that for the antiprotons, is well described by the calculations. Also the shift of the maximum in the \bar{p} spectra towards higher momenta is reproduced. A similar tendency can be observed if the cross sections from dC and αC reactions are compared to those from pC interactions. The heavier the observed particle the steeper the increase of the cross sections for the heavier projectiles, especially at the lowest incidence energies.

In order to make the presented results more obvious we show in figs. 2 and 3 the partial spectra from collisions of a projectile with b target nucleons

$$[a] + [b]$$

for the three projectile types and two selected ejectiles \bar{p} and π^+ . These partial spectra represent incoherent sums over contributions from all possible charge numbers, see (1), according to

$$d\sigma_{ab}(s) = \sum_{z_a=\max(0,a-\mathcal{Z}_A)}^{\min(a,\mathcal{Z}_A)} \sum_{z_b=\max(0,b-\mathcal{Z}_B)}^{\min(b,\mathcal{Z}_B)} \frac{dW(s; \boldsymbol{\alpha}_{az_a b z_b})}{\sum_{\boldsymbol{\alpha}_{az_a b z_b}} dW(s; \boldsymbol{\alpha}_{az_a b z_b})} .$$

The partial spectra result from the interplay between the values of the integrated partial cross sections

$$\sigma_{ab} = \sum_{z_a=\max(0,a-\mathcal{Z}_A)}^{\min(a,\mathcal{Z}_A)} \sum_{z_b=\max(0,b-\mathcal{Z}_B)}^{\min(b,\mathcal{Z}_B)} \sigma_{az_a b z_b} .$$

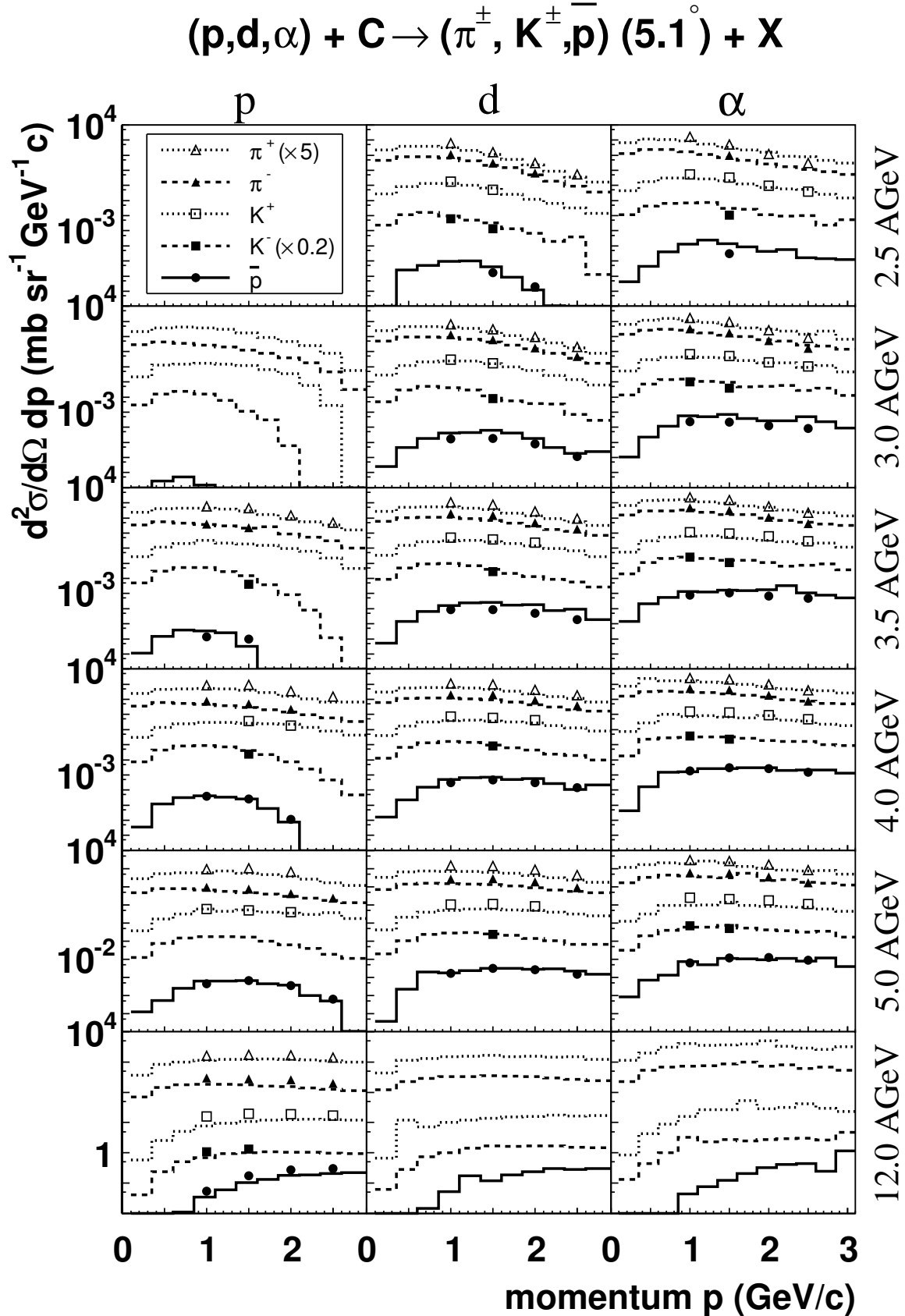


FIG. 1: Momentum spectra of π^\pm , K^\pm and \bar{p} [12] (symbols) from pC , dC and αC reactions compared with ROC-model calculations (histograms).

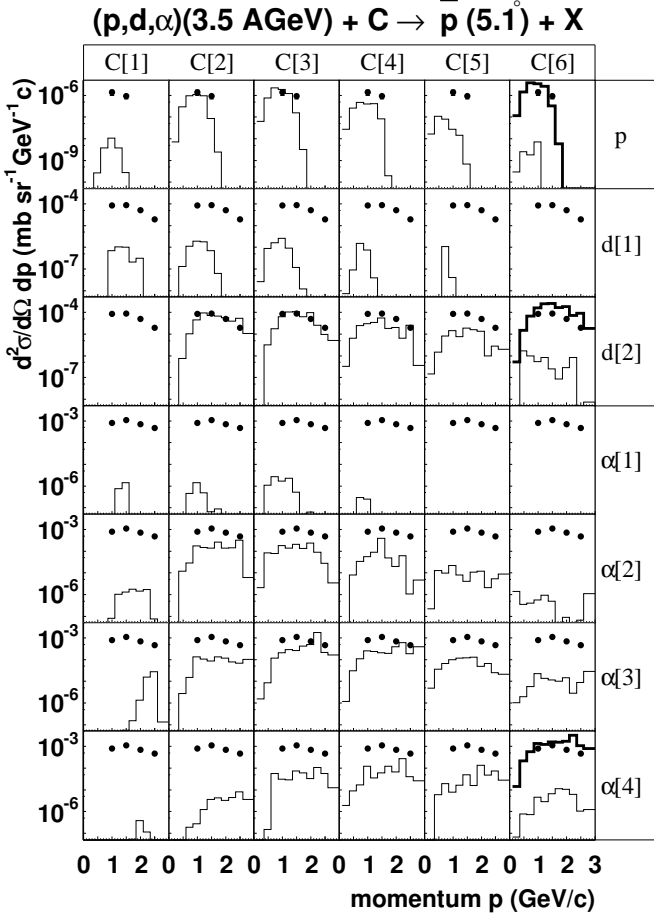


FIG. 2: Partial spectra of \bar{p} production calculated for pC , dC and αC reactions (thin histograms) compared to the data [12] (full circles). In six columns denoted by $C[b]$ the spectra from interactions with b participating target nucleons are plotted. Likewise, in the rows the numbers of participants in case of d - and α -induced reactions is denoted by $d[a]$ and $\alpha[a]$, respectively. The thick histograms are the sums of the partial spectra and coincide with the corresponding results from fig. 1.

and the energy dependence of the relative weights $dW(s; \alpha_{az_a b z_b})$ representing the production cross section in the $[a] + [b]$ interaction. In the case of $p + A$ reactions the σ_{1b} decrease monotonically with increasing number b of participating target nucleons, while for $A + A$ interactions symmetric combinations $a = b$ are preferred. Decisive for subthreshold particle production is the steep increase of the production cross section with the available energy above the threshold in the $[a] + [b]$ interaction under consideration. This explains the small contributions from the $[1] + [1]$ interactions, although σ_{11} represents for all projectile types the largest partial cross section. It is the small available energy which prevents higher \bar{p} production. With increasing number of participants both the mean available energy and the number of competing final channels increase. This results in maximal contri-

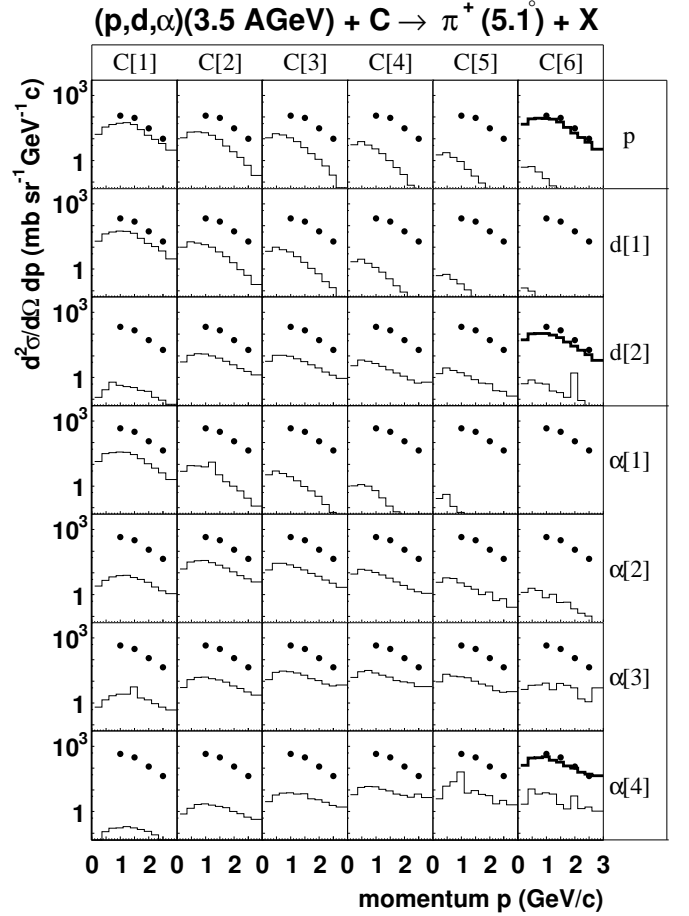


FIG. 3: The same as fig. 2 for π^+ .

butions from the combinations $[1] + [2]$ and $[1] + [3]$ in case of $p + A$ reactions. The spectral distributions are rather independent of the number of target participants b , see first row in fig. 2. This explains the successful description of the spectra in the “first-chance NN collision” approach, which corresponds to the $[1] + [1]$ process of the ROC-model, by appropriately selecting the normalisation [12]. Thus, the interpretation of the pC data by the ROC-model is quite contradictory to the assumptions of a “first-chance NN collision model”. Comparing the $[1] + [1]$ spectra from pC and dC reactions only a moderate increase of \bar{p} production is predicted by the ROC-model due to the Fermi motion in the deuteron. The enormous enhancement observed stems mainly from processes with both nucleons of the deuteron and several target nucleons involved where the energy available for particle production is much larger than in $[1] + [1]$ processes. In case of αC reactions the number of partial spectra contributing essentially increases. Here the larger available energy arises both from the larger masses of the interacting subsystems and from their internal motion in the projectile and the target. Thus one can conclude that from the viewpoint of the ROC-model the key quantity for understanding subthreshold particle production is the

number of participating nucleons. A direct experimental determination of this number for subthreshold \bar{p} production is highly desirable as discussed in [34] for the case of K^- production in pA reactions.

If we consider particle production far above the threshold as in fig. 3 then the main difference to subthreshold production consists in the higher value of the energy available for the production of the considered particle. This leads to a smoother energy dependence of the production cross section for the particle under consideration and the gain of available energy due to cluster-cluster processes does not play such an important role. In this way the partial spectra reflect primarily the values of the corresponding partial cross sections σ_{ab} with only minor corrections due to the energy dependence of the production cross section. Thus, the [1] + [1] processes with the largest partial cross section for all projectile types yield also the main contributions to the spectra.

IV. SUMMARY

Subthreshold particle production is a collective phenomenon which is far from being completely understood.

From the viewpoint of the ROC-model data on subthreshold particle production can be reproduced by considering the interaction of few-nucleon groups in complete analogy to the interaction of single nucleons, also with regard to high-momentum transfer processes. It has been demonstrated here that the cluster concept yields a quite natural explanation of the enhancement of subthreshold particle production due to the energy gain in the interaction of few-nucleon groups compared to NN interactions. This concept should be applicable not only in proton- or light-ion-induced reactions, but also for heavy-ion interactions, although in the latter case the number of partial processes increases tremendously. In this sense the ROC-model can be considered as a promising approach to a unified description of particle production processes in a large variety of different types of nuclear reactions.

Acknowledgments

One of the authors (H.M.) would like to thank W. Enghardt for the promotion of this study and A. Sibirtsev for useful discussions.

[1] O. Chamberlain et al., Phys. Rev. **100**, 947 (1955)
[2] O. Chamberlain et al., Nuovo Cimento **3**, 447 (1956)
[3] T. Elioff et al., Phys. Rev. **128**, 869 (1962)
[4] D. E. Dorfan et al., Phys. Rev. Lett. **14**, 995 (1965)
[5] A. Baldin et al., JETP Lett. **48**, 137 (1988)
[6] J. Carroll et al., Phys. Rev. Lett. **62**, 1829 (1989)
[7] A. Shor et al., Phys. Rev. Lett. **63**, 2192 (1989)
[8] A. Schröter et al., Nucl. Phys. A **553**, 775c (1993)
[9] A. Schröter et al., Z. Phys. A **350**, 101 (1994)
[10] Y. B. Lepikhin, V. A. Smirnitsky and V. A. Sheinkman, JETP Lett. **46**, 275 (1987)
[11] J. Chiba et al., Nucl. Phys. A **553**, 771c (1993)
[12] Y. Sugaya et al., Nucl. Phys. A **634**, 115 (1998)
[13] G. Q. Li et al., Phys. Rev. C **49**, 1139 (1994)
[14] G. Batko et al., Phys. Lett. B **256**, 331 (1991)
[15] S. W. Huang et al., Nucl. Phys. A **547**, 653 (1992)
[16] W. Cassing et al., Nucl. Phys. A **545**, 123c (1994)
[17] S. Teis et al., Phys. Lett. B **319**, 47 (1993)
[18] S. Teis et al., Phys. Rev. C **50**, 388 (1994)
[19] W. Cassing, G. Lykasov and S. Teis, Z. Phys. A **348**, 247 (1994)
[20] G. Batko et al., J. Phys. G **20**, 461 (1994)
[21] E. Hernández, E. Oset and W. Weise, Z. Phys. A **351**, 99 (1995)
[22] A. Sibirtsev et al., Nucl. Phys. A **632**, 131 (1998)
[23] P. Koch and C. B. Dover, Phys. Rev. C **40**, 145 (1989)
[24] C. M. Ko and X. Ge, Phys. Lett. B **205**, 195 (1988)
[25] C. M. Ko and L. H. Xia, Phys. Rev. C **40**, R1118 (1989)
[26] A. T. D'yachenko, J. Phys. G **26**, 861 (2000)
[27] P. Danielewicz, Phys. Rev. C **42**, 1564 (1990)
[28] V. I. Komarov, H. Müller and A. Sibirtsev, J. Phys. G. Submitted, nucl-th/0312087
[29] H. Müller, Z. Phys. A **353**, 103 (1995)
[30] H. Müller, Eur. Phys. J. C **18**, 563 (2001). hep-ph/0011350
[31] H. Müller and K. Sistemich, Z. Phys. A **344**, 197 (1992)
[32] H. Müller, Z. Phys. A **339**, 409 (1991)
[33] H. Müller, Z. Phys. A **353**, 237 (1995)
[34] H. Müller, Z. Phys. A **355**, 223 (1996)
[35] S. Shmakov, V. Uzhinskii and A. Zadorozhny, Comp. Phys. Communications **54**, 125 (1988)
[36] R. J. Glauber and J. Mathiae, Nucl. Phys. B **21**, 135 (1970)
[37] J. Knoll, Phys. Rev. C **20**, 773 (1979)
[38] S. Bohrmann and J. Knoll, Nucl. Phys. A **356**, 498 (1981)
[39] L. R. Elton, *Nuclear sizes/L. R. B. Elton*, London : Oxford Univ. Pr. (1961)
[40] M. Lacombe et al., Phys. Lett. B **101**, 139 (1981)
[41] A. S. Goldhaber, Phys. Lett. B **53**, 306 (1974)
[42] A. Shor, V. Perez-Mendez and K. Ganezer, Nucl. Phys. A **514**, 717 (1990)
[43] J. V. Geaga et al., Phys. Rev. Lett. **45**, 1993 (1980)
[44] C. Ciofi degli Atti and S. Simula, Phys. Rev. C **53**, 1689 (1996)
[45] O. Benhar, A. Fabrocini and S. Fantoni, Nucl. Phys. A **505**, 267 (1989)
[46] I. Sick et al., Phys. Lett. B **323**, 267 (1994)
[47] A. Sibirtsev, W. Cassing and U. Mosel, Z. Phys. A **358**, 357 (1997)
[48] E. Byckling and K. Kajantie, *Particle Kinematics*, John Wiley and Sons, London, New York, Sydney, Toronto (1973)
[49] G. Westfall et al., Phys. Rev. C **17**, 1368 (1978)
[50] J. Bondorf et al., Nucl. Phys. A **443**, 321 (1985)
[51] V. V. Anisovich and V. M. Shekhter, Nucl. Phys. B **55**, 455 (1973)

- [52] C. Caso et al., *Eur. Phys. J. C* **3**, 1 (1998)
- [53] B. Andersson et al., *Phys. Rep.* **97**, 31 (1983)
- [54] B. Andersson, G. Gustafson and B. Nilsson-Almqvist, *Nucl. Phys. B* **281**, 289 (1987)
- [55] T. Sjöstrand and M. van Zijl, *Phys. Rev. D* **36**, 2019 (1987)
- [56] T. Sjöstrand, *Comput. Phys. Commun.* **82**, 74 (1994)